Reduction of Interstitial Cells of Cajal in Esophageal Atresia

*Paola Midrio, †Rita Alaggio, *Aleksandra Strojna, *Piergiorgio Gamba, †Luciano Giacomelli, †Sara Pizzi, and ‡Maria Simonetta Faussone-Pellegrini

ABSTRACT

Objectives: Postrepair esophageal dysmotility and gastroesophageal reflux are well-known consequences in patients with congenital esophageal atresia (EA) with or without distal tracheoesophageal fistula (TEF). The interstitial cells of Cajal (ICC), considered the intestinal pacemaker, are altered in congenital diseases with abnormal peristalsis, but no data are available for EA. Therefore, presence and maturation of ICC was verified in EA-TEF newborns.

Patients and Methods: Fifteen full-term neonates underwent repair of EA-TEF. Control specimens were from 10 newborns who died of nonesophageal diseases. Specimens from upper pouch, fistula, proximal, and distal esophagus were processed for hematoxylin and eosin, c-kit immunohistochemistry for ICC identification, and transmission electron microscopy. Frequency of c-kit–positive cells was evaluated in 20 fields per slide using a visual score (absent, very low, low, medium, high, very high). Morphocytometry and statistical analysis were also performed.

Results: In the proximal normal esophagus, ICC frequency was very high (3 cases), high (5), and medium (2); distally, it was high (4) and medium (6). In EA-TEF upper pouch, it was high (2) and medium (13); in the fistula, it was medium (5), low (6), very low (3), and absent (1). Morphocytometry confirmed these results. Comparison between pouch and fistula versus proximal and lower esophagus, respectively, showed statistically significant differences. Transmission electron microscopy demonstrated ICC immaturity in EA-TEF.

Conclusions: The significant lower ICC density in EA-TEF is in favor for the pathogenesis of esophageal dysmotility frequently observed in such patients.

Key Words: esophageal atresia, interstitial cells of Cajal, tracheoesophageal fistula

(*JPGN* 2010;51: 610–617)

Esophageal atresia (EA) with tracheoesophageal fistula (TEF) is a congenital malformation in which, despite a successful surgical approach, the peristalsis can be subsequently altered requiring medical and surgical treatments. Different factors may be responsible for this condition, including type of EA (1), gap between upper and lower pouches (2), intraoperative mobilization and denervation (3), and associated malformations (4). All of these factors may contribute to the onset of gastroesophageal reflux (GER), which is a common well-known consequence of patients with EA. Morbidity of this condition may require a further surgical intervention if it is not responsive to medical treatment (5–7).

The beginning and the end of the digestive tract, that is pharynx and rectum, respectively, are the only intestinal segments with a striated voluntary muscle coat. The remaining intestine presents an involuntary smooth muscle coat whose peristalsis is modulated by the ganglia of the autonomous nervous system located between the muscle layers. The interstitial cells of Cajal (ICC), first described by Cajal at the end of the 19th century (8), are an integrating part of this system and are able to generate and propagate intestinal peristalsis (9–11). They form networks distributed around myenteric (Auerbach) plexus elements (the so-called myenteric ICC [ICC-MY]) and within the intramuscular layers (the so-called intramuscular ICC [ICC-IM]), and determine electrical and mechanical activities of smooth muscle cells (12). The abnormal distribution, maturation, and number of the ICC have already been reported in several pediatric diseases whose peristalsis is impaired, such as chronic idiopathic intestinal pseudoobstruction (13,14), Hirschsprung disease (15,16), neuronal intestinal dysplasia (17), infantile hypertrophic pyloric stenosis (18,19), and gastroschisis (20,21).

In the literature, there are data describing the ICC in the normal human esophagus (22,23), but none is available for the presence and distribution of ICC in the case of EA. The purpose of the present study was to investigate the distribution and maturation of the ICC in the upper pouch and distal fistula in a consecutive series of newborns affected by EA-TEF.

PATIENTS AND METHODS

Full-thickness tissue samples from 15 term neonates undergoing surgery for EA with distal TEF (EA-TEF) were collected at the tip of the upper pouch and tip of the tracheal fistula. Mean gestational age was 38.6 weeks (range 38–41.2); premature newborns were excluded from the study because the maturation and distribution of the ICC before the 38th week of pregnancy are incomplete (24). Mean birth weight was 3390 g (range 2900–3725 g), associated malformations were present in 4 cases (2 cardiac, 1 renal and anorectal, 1 vertebral), and no chromosomal anomalies were detected. The mean age at the time of surgery was 20 hours (range 10–46 hours). The mean gap between pouches was 1.7 cm (range 1.5–2 cm). Normal controls, represented by esophageal biopsies collected at the level of the carina (for the proximal esophagus) and 4 cm more distally (for the inferior esophagus), were obtained from 10 full-term newborns who died of nonesophageal diseases (8 with cardiac malformations, 2 with intraventricular hemorrhage). The mean age at the time of death was 60 hours (range 1–480 hours).

Received July 9, 2009; accepted March 13, 2010.

From the *Division of Paediatric Surgery, the †Department of Pathology, University of Padua, and the ‡Department of Anatomy, Histology and Forensic Medicine, University of Florence, Italy.

Address correspondence and reprint requests to Paola Midrio, MD, Ospedale Civile, Department of Paediatrics, Paediatric Surgery, Via Giustiniani 3, 35121 Padova, Italy (e-mail: midrio@pediatria.unipd.it).

The authors report no conflicts of interest.

DOI: 10.1097/MPG.0b013e3181dd9d40

Immunohistochemistry

Tissue specimens were fixed in 10% neutral formalin and embedded in paraffin. Consecutive slides of 4-μm thickness were deparaffined by xylene, dehydrated through ascending grades of alcohol to water (1 × 5 minutes each), cleared in Histoclear (2 × 5 minutes), and left in molten wax at 56°C before embedding. To determine the presence of the ICC, a rabbit polyclonal primary antibody against c-kit was used (DAKO, dilution 1:300, Glostrup, Denmark). Immunolabeling was obtained by using the detection Kit-Polymer (NovoLink Polymer Detection System, 500 tests, Novocastra, UK) according to the manufacturer's instructions. The endogenous peroxidase was inhibited by Novocastra Peroxydase Block RE7101 Kit, followed by the protein block by Novocastra Protein Block RE7102. This was followed by incubation with the primary antibody for 45 minutes at room temperature, rinsing in phosphate-buffered saline, incubation with the postprimary block RE7111 for 20 minutes at room temperature, and final incubation with NovoLink Polymer RE7112 for 20 minutes at room temperature. Immunoreactivity was detected at room temperature by the addition of 3,3′-diaminobenzidine (DAB, Novocastra, Newcastle upon Tyne, UK) as a substrate. After immunostaining, the specimens were counterstained with hematoxylin. Negative control was obtained by omitting the corresponding primary antibody.

A semiquantitative analysis of the frequency of ICC was performed by 2 independent pathologists, both experts in ICC, using a ''visual score'' (Table 1). Both ICC-IM and ICC-MY were examined: to analyze the ICC-IM, 20 fields per slide were randomly chosen under light microscopy at high-power field (×40). Moreover, 5 to 10 ganglia of the myenteric plexus were also randomly chosen to evaluate the ICC-MY. Scattered mast cells were found and used as positive internal control.

Morphocytometry

The same microscopic fields were also used to perform the semiquantitative analysis by morphocytometry. The ''CYRES'' system for image analysis (Zeiss, Jena, Germany), including a conventional microscope (I model Axioscope, Zeiss) and a 2-color camcorder 3CCD (KY-F%BE, JVC, Yokohama, Japan), was used. The images were acquired by means of a frame grabber (Kotron, Eching, Germany) and subsequently analyzed. The frame grabber and the program for image analysis, operating simultaneously with the video camera, were connected to a computer. The intensity of illumination remained unchanged during each measurement. Results were expressed as area fraction media (a percentage of area occupied by c-kit positivity). The number of mast cells was limited in 4 specimens of EA-TEF and very high in just 1 case. The positivity of the mast cells was manually excluded.

TABLE 1. Visual score for frequency of ICC-IM and ICC-MY

Grade 0 = absent (complete absence of ICC)
Grade I = very low (isolated positive cells)
Grade II = low (scattered positive cells)
Grade III = medium (patchy distribution of positive cells with initial formation of a network)
Grade IV = high (numerous positive cells detected also at low-power field with formation of a network in some microscopic fields)
Grade V = very high (numerous positive cells, with evidence of a well-formed network in the majority of microscopic fields)

ICC = interstitial cells of Cajal; ICC-IM = intramuscular ICC; ICC-MY = myenteric ICC.

Transmission Electron Microscopy

Full-thickness specimens of the upper pouch and fistula, obtained from a patient with EA-TEF, and of the upper and distal part of the esophagus, obtained from a baby who died at 48 hours of life of nonesophageal disease, were immersed in a fixative solution of 2% cacodylate-buffered glutaraldehyde (pH 7.4) for 6 hours. They were then rinsed in cacodylate buffer supplemented with 15% sucrose, postfixed with 1% phosphate-buffered OsO_4 (pH 7.4) for 2 hours, dehydrated with graded alcohol, clarified in propylene oxide, and embedded in Epon using flat molds. Semithin sections were cut with an LKB NOVA ultramicrotome (LKB Vertriebs GmbH, Vienna, Austria), stained with a solution of toluidine blue in 0.1 mol/L borate buffer, and then observed under a light microscope. Ultrathin sections of the selected areas were obtained with the same ultramicrotome using a diamond knife and stained with uranyl acetate, followed by a solution of concentrated bismuth subnitrate. The sections were examined under a JEOL 1010 electron microscope (JEOL Ltd, Tokyo, Japan) and photographed.

Statistical Analysis

The STATA version 8.1 software package (StataCorp, College Station, TX) was used for statistical data analyses. Data are expressed as median with standard deviation (SD). The Fisher exact test, Pearson χ^2 test, and Wilcoxon rank sum test were used for univariate comparisons between 2 groups.

Spearman rank correlation was applied to assess the agreement between both pathologists. A P value of <0.05 was considered statistically significant for all of the evaluations.

RESULTS

Immunohistochemistry

Immunostaining showed a distribution of c-kit–positive cells across the entire circular muscle layer, at the myenteric plexus level, and the longitudinal muscle layer. In the muscle layers of normal esophagus, the ICC-IM appeared with fusiform body, frequently with a typical bipolar morphology, interconnected to each other, and extending parallel to the muscle bundles (Fig. 1A–C). In the myenteric plexus area, the ICC-MY were usually fusiform with short and branched cytoplasmic expansion to form a rich cellular net around the ganglia (Fig. 2A).

The ICC-IM in the atretic esophagus frequently appeared separated, with a narrow body, nonoriented, and often devoid of branched processes (Fig. 1B and D). The ICC-MY were rare, exceptionally detected, or completely absent (Fig. 2B). This marked decrease of ICC-MY was associated with an equivalent reduction, or absence, of myenteric plexus ganglia.

Evaluation by Visual Score

The grade of agreement between pathologists, calculated with Spearman correlation, was 85% (range 65%–97%).

Controls

The ICC-IM score (Table 2) in the proximal esophagus was grade V (very high) in 3 specimens (30%), grade IV (high) in 5 (50%), and grade III (medium) in 2 (20%). In the distal esophagus,

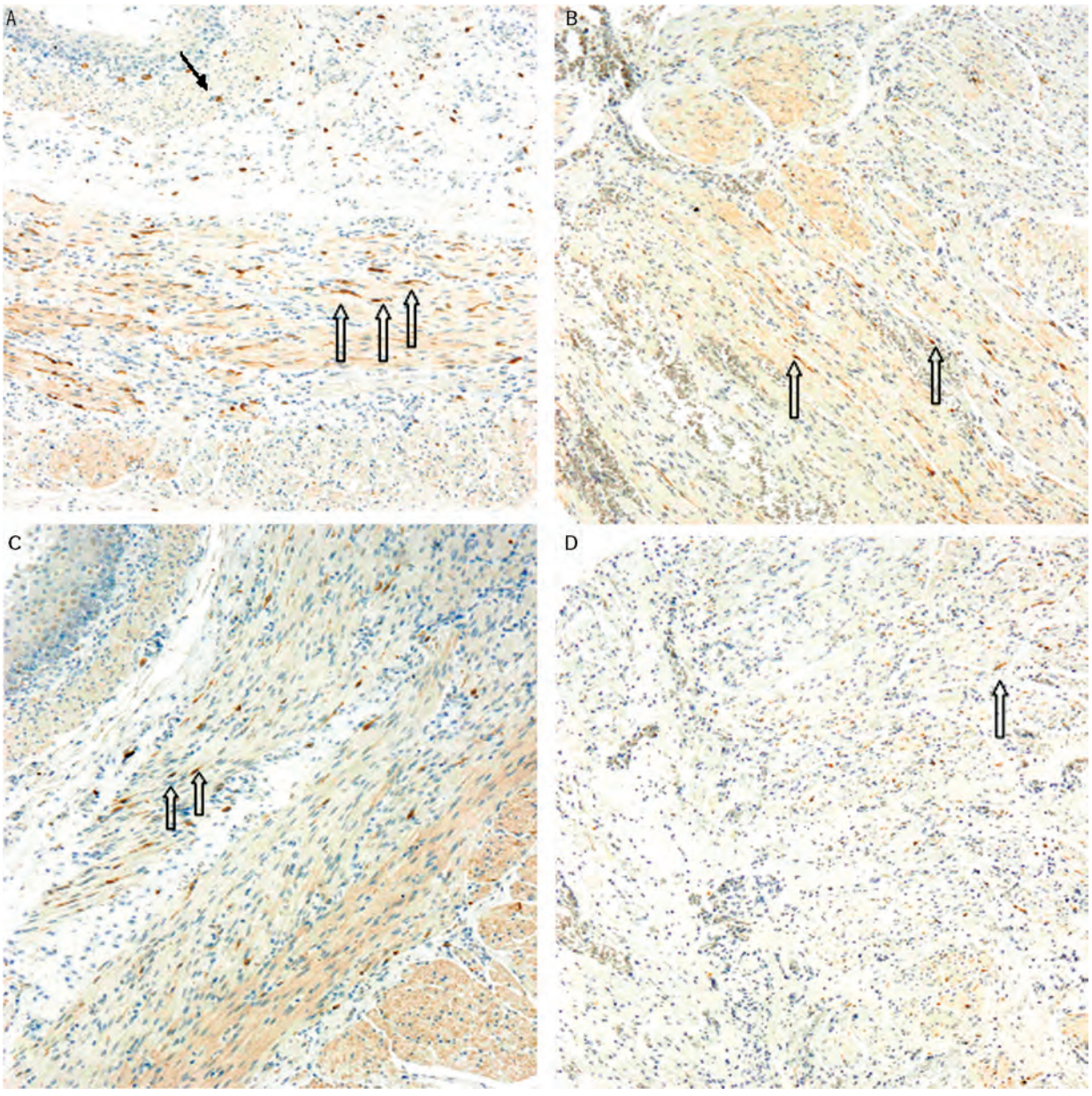

FIGURE 1. (A) Proximal and (C) distal normal esophagus (original magnification ×80). ICC-IM show the typical bipolar morphology and are connected to each other forming a network parallel to the inner muscular layer in proximal esophagus (open arrows). Scattered mast cells are present in the lamina propria (A, black arrow). In the distal esophagus, the ICC-IM are less numerous but equally connected to each other (C, open arrows). Atretic esophagus: upper pouch (B) and fistula (D). Scattered and nonoriented ICC-IM are found in the upper pouch (B, open arrows); in the fistula (D), the ICC-IM are further reduced in number (open arrow). ICC-IM = intramuscular interstitial cells of Cajal.

4 specimens (40%) showed a score IV and 6 (60%) showed a score III. The frequency of ICC-IM was significantly higher in the proximal esophagus compared with the distal one ($P = 0.013$). There was, indeed, a craniocaudal gradient of ICC-IM concentration when considering each normal esophagus separately (as data in Table 2, reporting frequency of ICC-IM, may suggest).

The ICC-MY (Table 3) score in the proximal esophagus was III in 1 case (10%), II in 5 (50%), and I in 4 (40%). In the distal esophagus, 1 specimen (10%) showed a score III, 3 (30%) score II, and 6 (60%) score I. Also, the frequency of ICC-MY was higher in the proximal esophagus compared with the distal one; however, this difference was not statistically significant ($P = 0.89$).

EA-TEF Cases

The semiquantitative grading of ICC-IM (Table 2) revealed in the upper pouch a grade IV (high) in 2 specimens (13.3%) and

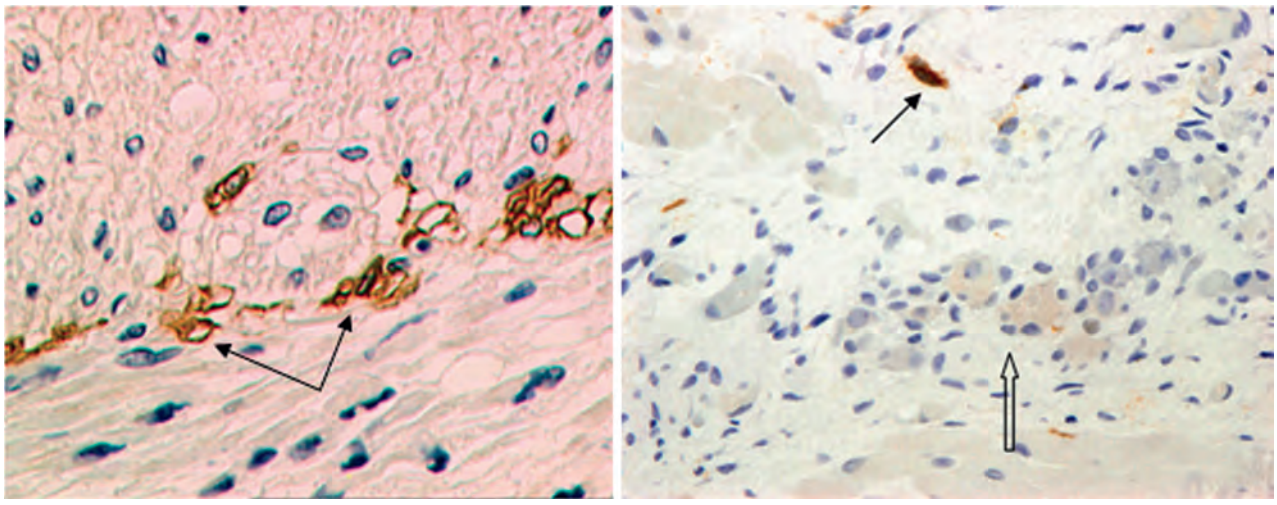

FIGURE 2. Distribution of ICC-MY at the myenteric plexus level (original magnification ×320). The ICC-MY form a rich cellular network around the ganglion in the normal esophagus (A) (black arrows). In the atretic esophagus (B), the ICC-MY are absent around the ganglion (open arrow), in the presence of a positive internal control represented by c-kit–positive mast cells (black arrow). ICC-IM = intramuscular interstitial cells of Cajal.

grade III (medium) in 13 (86.7%). The frequency of ICC-IM in the fistula was of grade III (medium) in 5 cases (33.3%), grade II (low) in 6 (40%), grade I (very low) in 3 (20%), and grade 0 (absent) in 1 (6.7%). The frequency of ICC-IM was significantly higher in the upper pouch compared with the fistula ($P = 0.0001$) with a craniocaudal gradient when considering each EA-TEF separately.

The semiquantitative grading of ICC-MY (Table 3) revealed a grade 0 (absent) in 8 upper pouches (53%) and in 11 fistulas (73%). A grade I was attributed in 7 upper pouches (47%) and 4 fistulas (27%). There were no significant differences between upper pouch and fistula samples ($P = 0.658$).

When the mean frequency of ICC in the proximal esophagus was compared with the mean frequency in the upper pouch, it was significantly greater ($P = 0.0002$). Similarly, the mean frequency of ICC in the distal esophagus was statistically greater compared with the mean frequency in the fistula ($P = 0.0015$). Overall, the c-kit positivity was significantly reduced in EA compared with controls.

Evaluation by Morphocytometry

The morphocytometric results are reported in Table 4 and confirmed those obtained with the visual score. In EA, the mean frequency of ICC (expressed as a percentage of area occupied by c-kit positivity) was 17.92 (SD 9.89) and 7.97 (SD 7.33) in the upper pouch and fistula, respectively. In normal esophagus, the mean frequency of ICC was 30.65 (SD 12.92) and 18.04 (SD 7.68) in the proximal and distal parts, respectively.

Also with this method, when the mean frequency of ICC in the proximal esophagus was compared with the mean frequency in the upper pouch, it was significantly greater ($P = 0.001$). Similarly, the mean frequency of the ICC in the distal esophagus was statistically greater compared with the mean frequency in the fistula ($P = 0.003$).

Transmission Electron Microscopy

In both cases, atretic and control subjects, the tissue was poorly preserved and showed clear signs of hypoxia; however, it

TABLE 2. Frequency of ICC-IM evaluated by visual score in EA-TEF (upper pouch and fistula) and controls (proximal and distal esophagus)

			Controls	
Visual score	EA-TEF upper pouch	EA-TEF fistula	Proximal esophagus	Distal esophagus
G.0 = absent	0	1	0	0
G.I = very low	0	3	0	0
G.II = low	0	6	0	0
G.III = medium	13	5	2	6
G.IV = high	2	0	5	4
G.V = very high	0	0	3	0
Mean	3.1	2.0	4.1	3.4
SD	0.4	0.9	0.7	0.5
Total specimens	15	15	10	10

Grades 0 to III are considered as low density of ICC. EA-TEF = esophageal atresia-tracheoesophagel fistula; ICC-IM = intramuscular interstitial cells of Cajal.

TABLE 3. Frequency of ICC-MY evaluated by visual score in EA-TEF (upper pouch and fistula) and controls (proximal and distal esophagus)

			Controls	
Visual score	EA-TEF upper pouch	EA-TEF fistula	Proximal esophagus	Distal esophagus
G.0 = absent	8	11	0	0
G.I = very low	7	4	4	6
G.II = low	0	0	5	3
G.III = medium	0	0	1	1
G.IV = high	0	0	0	0
G.V = very high	0	0	0	0
Mean	0.46	0.26	1.7	1.5
SD	0.51	0.45	0.67	0.7
Total specimens	15	15	10	10

EA-TEF = esophageal atresia-tracheoesophagel fistula; ICC-MY = myenteric interstitial cells of Cajal.

was possible to evaluate the presence of cells with fibroblastic features, having a more or less developed rough endoplasmic reticulum, an elongated shape, and lateral processes. These cells were located between striated muscle fibers in the upper pouch (Fig. 3A and B) and smooth muscle cells in the fistula (Fig. 3C). In the control, the putative ICC were characteristically close to both smooth muscle cells and nerves (Fig. 3D) and showed a clear cytoplasm containing intermediate filaments. Caveolae were only occasionally seen and none of these cells was rich in rough endoplasmic reticulum cisternae.

DISCUSSION

The present study examined both ends of the most common type of EA, that is EA-TEF, and in particular, for the first time, the ICC, which are an important player in peristalsis, both with immunohistochemistry and TEM. The ICC were first described in the intestine by Cajal at the end of the 19th century (8), but only 100 years later was their role of intestinal pacemaker defined (9).

This study demonstrates that these cells were significantly reduced in EA compared with controls and some further considerations can be drawn from the immunohistochemistry analysis. First, there is a difference in the number of c-kit–positive cells (ie, the ICC) between controls and atretic esophagi, the former being significantly more numerous than the latter, especially those at the myenteric plexus that are the ICC type mainly involved in peristalsis. This datum is more evident with the visual score analysis than with morphocytometry. The marked decrease of ICC-MY is associated with an equivalent reduction, or absence, of myenteric plexus ganglia. This datum is in accord with the observations from other authors (25,26). Second, an altered morphology of the ICC, together with their reduction, did not allow in patients with EA the formation of the ICC networks whose integrity is fundamental for correct motility (10,11).

Moreover, we observed a craniocaudal distribution of the ICC in both controls and cases, being more numerous in the upper esophagus and proximal pouch compared with the distal esophagus and fistula, respectively. None of the previous experimental and human articles, either describing the intrinsic or extrinsic esophageal innervation, has ever reported this datum. The observation that a craniocaudal distribution of c-kit–positive cells seems present along the esophagus is intriguing. The aboral progression of neural crest–derived cells leaves the distal part with less concentration of neuronal cells also in controls with a consequent retarded maturation of their target cells, the ICC (23). In case of interruption of the organ's continuity, as it occurs in EA, it is reasonable to believe this progression of neural crest–derived cells is hampered, leaving the distal part with a very low concentration of neuronal cells and, consequently, leading to defective maturation of the ICC. This may lead to an impaired peristalsis that, together with a more or less extended surgical procedure, may ultimately be responsible for the occurrence of GER.

TEM analysis confirmed the results obtained with immunohistochemistry. The ICC of controls, although poorly preserved, showed typical features and characteristic relations with both smooth muscle cells and nerve endings. The ICC of the upper esophagus in atretic patients were immature, with fibroblast-like features (21,23). Very immature ICC or ICC precursors (when fibroblastic-like features are present) are, indeed, c-kit negative (20,27). In atretic patients, therefore, the differentiation of ICC is delayed and this may justify the scarcity of the c-kit–positive cells, as highlighted by immunohistochemistry.

All of these findings may fit well with 1 of the most common sequelae following EA repair, which is GER. This is a long-standing matter, with the first report dating back to 1957 (28), and, although it is a well-known event in the follow-up of EA (5,29), the exact etiology remains uncertain and probably multifactorial, including an impaired esophageal peristalsis and altered lower

TABLE 4. Mean frequency of interstitial cells of Cajal evaluated by morphocytometry

	A	B	C	D
Morphocytometry (SD)	17.92 (9.89)	7.97 (7.33)	30.65 (12.92)	18.04 (7.68)
Comparison	A to C	B to D		
P	0.001	0.003		

A = EA-upper pouch; B = EA-fistula; C = proximal esophagus; D = distal esophagus.

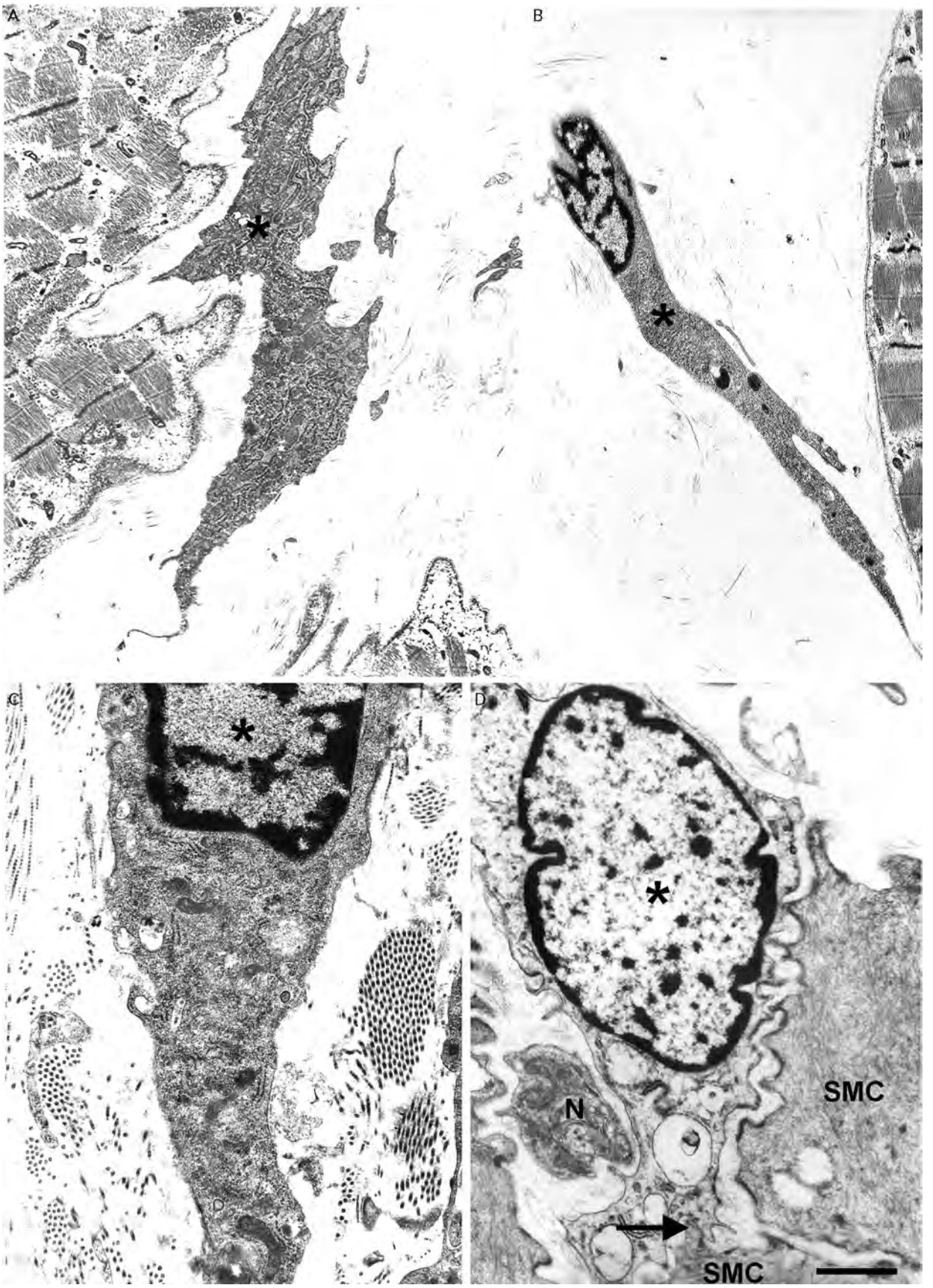

esophageal sphincter. As already observed (30), it may be hard or impossible to understand whether the main cause of abnormal esophageal motility is surgical damage to the nerve fibers that innervate the esophagus or a congenital abnormality of neuromuscular components. It was, indeed, reported that GER and uncoordinated peristalsis were detected in the preoperative studies of patients with H-type TEF (31), suggesting the esophageal neuromuscular components may be congenitally altered. Ever since, a series of experimental and clinical articles studied how different factors may be involved in the postoperative esophageal dysfunction of EA.

In the EA rat model, both the extrinsic nerves and intrinsic intramural nervous components of the esophagus were examined (30,32). In this model, it was noted that the left vagus nerve joined the right one after tracheal bifurcation and no esophageal plexus was present in the lower esophagus; therefore, it was speculated that relatively few branches of both vagi penetrated the lower esophagus (30). The same author also reported a significantly reduced density of nerve plexus, ganglia, and cell bodies per ganglion in the atretic esophagus of rat fetuses (32) that may further contribute to the postoperative dysmotility. Cheng et al (33) found the nerve tissue, which normally encircles the esophagus, was thinner and shorter in fetuses with EA compared with controls and nerve distribution was reduced by 50%. This, theoretically, may lead to a decreased innervation of the esophageal musculature and, ultimately, be related to the esophageal dysmotility.

A series of articles on human EA paralleled the experimental data. One of the first observations comes from Nakazato et al (34) who reported on 5 polimalformed patients with EA and TEF, dead before surgical correction. With the microdissection technique they found a lower fraction of neural tissue in the layer of the Auerbach plexus in the atretic esophagus compared with controls. The authors suggested this deficiency in Auerbach plexus, more evident in the lower esophagus, could contribute to dysphagia and GER in patients with EA-TEF. Boleken et al (25) examined only the proximal end of 9 atretic esophagi and concluded there were marked hypoganglionosis and deficient distribution of immature ganglion cells and some nerve fibers in EA, together with a compensatory hypertrophied glial tissue. Li et al (26), instead, studied the intrinsic innervation only in the fistula of patients with EA-TEF with TEM and immunohistochemistry. They found an abnormal intrinsic dysplasia of myenteric nerve plexus and an imbalanced release of neurotransmitters, in particular an increased expression of inhibitory neuropeptides, such as vasoactive intestinal polypeptide and nitric oxide. Altogether these findings may be in charge for the postoperative esophageal dysfunction, such as the abnormal relaxation of the esophageal smooth muscle. Dutta et al (35) also examined the fistula and found an abnormal number of glands, ducts, and mucins whose clinical significance, however, remains unclear. Pederiva et al (36) analyzed the intrinsic innervation of both proximal and distal esophageal segments of a much rarer variant of EA, that is EA without fistula. They found larger intramural ganglia with larger cells and, with the antineurofilament immunostaining, a denser intracytoplasmatic fibrillar network in patients with EA compared with age-unmatched controls. They concluded these neural anomalies are in part similar to those described in the most common EA-TEF. Although these studies are not homogeneous with regards to examined samples and type of EA, they may contribute, from different points of view, to the unclear problem of GER following EA repair.

CONCLUSIONS

In summary, the number of patients is too small to draw any definitive conclusions; however, this investigation provides some new and important information about number and differentiation of ICC, the cells involved in the peristalsis, thus adding another piece to the complex puzzle of the postoperative dysmotility of patients with EA.

REFERENCES

1. Engum SA, Grosfeld JL, West KW, et al. Analysis of morbidity and mortality in 227 cases of esophageal atresia and/or tracheoesophageal fistula over two decades. *Arch Surg* 1995;130:502–9.
2. Lopes MF, Botelho MF. Midterm follow-up of esophageal anastomosis for esophageal atresia repair: long-gap versus non-long-gap. *Dis Esophagus* 2007;20:428–35.
3. Shono T, Suita S, Arima T, et al. Motility function of the esophagus before primary anastomosis in esophageal atresia. *J Pediatr Surg* 1993; 28:673–6.
4. Brown AK, Roddam AW, Spitz L, et al. Oesophageal atresia, related malformations, and medical problems: a family study. *Am J Med Genet* 1999;85:31–7.
5. Krug E, Bergmeier JH, Dees J, et al. Gastroesophageal reflux and Barrett's esophagus in adults born with esophageal atresia. *Am J Gastroenterol* 1999;94:2825–8.
6. Somppi E, Tammela O, Ruuska T, et al. Outcome of patients operated on for esophageal atresia: 30 years' experience. *J Pediatr Surg* 1998;33: 1341–6.
7. Bergmeijer J, Tibboel D, Hazebroek FW. Nissen fundoplication in the management of gastroesophageal reflux occurring after repair of esophageal atresia. *J Pediatr Surg* 2000;35:573–6.
8. Cajal SR. Sur les ganglions et plexus nerveux de l'intestin. *C R Soc Biol (Paris)* 1893;45:217–23.
9. Maeda H, Yamataka A, Nishikawa S, et al. Requirement of c-kit for development of intestinal pacemaker system. *Development* 1992;116: 369–75.
10. Sanders KM, Ward SM. Interstitial cells of Cajal—a new perspective on smooth muscle function. *J Physiol* 2006;576:721–6.
11. Huizinga JD, Thuneberg L, Kluppel M, et al. W/kit gene required for interstitial cells of Cajal and for intestinal pacemaker activity. *Nature* 1995;373:347–9.
12. Faussone-Pellegrini MS, Thuneberg L. Guide to the identification of interstitial cells of Cajal. *Microsc Res Tech* 1999;47:248–326.
13. Streutker CJ, Huizinga JD, Campbell F, et al. Loss of CD117 (c-kit)- and CD34-positive ICC and associated CD34-positive fibroblasts defines a subpopulation of chronic intestinal pseudo-obstruction. *Am J Surg Pathol* 2003;27:228–35.
14. Yamataka A, Ohshiro K, Kobayashi H, et al. Abnormal distribution of intestinal pacemaker (C-KIT-positive) cells in an infant with chronic idiopathic intestinal pseudoobstruction. *J Pediatr Surg* 1998;33:859–62.

FIGURE 3. (A–C) Atretic esophagus and (D) control. (A) Upper pouch. A large-sized cell (asterisk) with fibroblastic-like features, as demonstrated by the abundant cytoplasm rich in mitochondria and cisternae of the rough endoplasmic reticulum. This cell is located close to a striated muscle fiber, and has an elongated shape and many short lateral processes. (B) Upper pouch. A thin spindle-shaped cell (asterisk) located in the proximity of a striated muscle fiber, having few cisternae of rough endoplasmic reticulum, and showing only 1 lateral process. (C) Fistula. Detail of a cell (asterisk) with features similar to those in (A) and (B). This cell is located close to smooth muscle cells and immersed in a fibrotic connective tissue. (D) Control distal esophagus. Interstitial cells of Cajal (ICC) (asterisk) close to a nerve fiber (N) and in contact (arrow) with a smooth muscle cell (SMC). This ICC has a clear cytoplasm and very few cisternae of rough endoplasmic reticulum. Scale bar: A and D = 1 μm; B = 1.6 μm; C = 0.6 μm.

15. Matsuura KTK, Matsuoka T, Nakatani H, et al. A morphological study of the pacemaker cells of the aganglionic intestine in Hirschsprung's disease utilizing ls/ls model mice. *Med Mol Morphol* 2005;38:123–9.
16. Wedel T, Spiegler J, Soellner S. Enteric nerves and interstitial cells of Cajal are altered in patients with slow-transit constipation and megacolon. *Gastroenterology* 2002;123:1459–67.
17. Jeng YM, Mao TL, Hsu WM, et al. Congenital interstitial cell of Cajal hyperplasia with neuronal intestinal dysplasia. *Am J Surg Pathol* 2000;24:1568–72.
18. Vanderwinden J, Liu H, Menu R, et al. The pathology of infantile hypertrophic pyloric stenosis after healing. *J Pediatr Surg* 1996;31:1530–4.
19. Vanderwinden J, Liu H, De Laet M, et al. Study of the interstitial cells of Cajal in infantile hypertrophic pyloric stenosis. *Gastroenterology* 1996;111:279–88.
20. Midrio P, Faussone-Pellegrini MS, Vannucchi MG, et al. Gastroschisis in the rat model is associated with a delayed maturation of intestinal pacemaker cells and smooth muscle cells. *J Pediatr Surg* 2004;39:1541–7.
21. Midrio P, Vannucchi MG, Pieri L, et al. Delayed development of interstitial cells of Cajal in the ileum of a human case of gastroschisis. *J Cell Mol Med* 2008;12:471–8.
22. Faussone-Pellegrini MS. Histogenesis, structure and relationships of interstitial cells of Cajal (ICC): from morphology to functional interpretation. *Eur J Morphol* 1992;30:137–48.
23. Faussone-Pellegrini MS, Cortesini C. Ultrastructural features and localization of the interstitial cells of Cajal in the smooth muscle coat of human esophagus. *J Submicrosc Cytol Pathol* 1985;17:187–97.
24. Faussone-Pellegrini MS, Vannucchi MG, Alaggio R, et al. Morphology of the interstitial cells of Cajal of the human ileum from foetal to neonatal life. *J Cell Mol Med* 2007;11:482–94.
25. Boleken M, Demirbilek S, Kirimiloglu H, et al. Reduced neuronal innervation in the distal end of the proximal esophageal atretic segment in cases of esophageal atresia with distal tracheoesophageal fistula. *World J Surg* 2007;31:1512–7.
26. Li K, Zheng S, Xiao X, et al. The structural characteristics and expression of neuropeptides in the esophagus of patients with congenital esophageal atresia and tracheoesophageal fistula. *J Pediatr Surg* 2007;42:1433–8.
27. Kenny SE, Vanderwinden JM, Rintala RJ, et al. Delayed maturation of the interstitial cells of Cajal: a new diagnosis for transient neonatal pseudoobstruction. Report of two cases. *J Pediatr Surg* 1998;33:94–8.
28. Haight C. Some observations on esophageal atresia and tracheoesophageal fistulas of congenital origin. *J Thorac Cardiovasc Surg* 1957;34:141–72.
29. Deurloo JA, Ekkelkamp S, Bartelsman JFWM, et al. Gastroesophageal reflux: prevalence in adults older than 28 years after correction of esophageal atresia. *Ann Surg* 2003;238:686–9.
30. Qi BQ, Merei J, Farmer P, et al. The vagus and recurrent laryngeal nerves in the rodent experimental model of esophageal atresia. *J Pediatr Surg* 1997;32:1580–6.
31. Romeo G, Zucarello B, Proietto F, et al. Disorders of the esophageal motor activity in atresia of the esophagus. *J Pediatr Surg* 1987;22:120–4.
32. Qi BQ, Uemura S, Farmer P, et al. Intrinsic innervation of the oesophagus in fetal rats with oesophageal atresia. *Pediatr Surg Int* 1999;15:2–7.
33. Cheng W, Bishop AE, Spitz L, et al. Abnormal enteric nerve morphology in atretic esophagus of fetal rats with adriamycin-induced esophageal atresia. *Pediatr Surg Int* 1999;15:8–10.
34. Nakazato Y, Landing BH, Wells TR. Abnormal Auerbach plexus in the esophagus and stomach of patients with esophageal atresia and tracheoesophageal fistula. *J Pediatr Surg* 1986;21:831–7.
35. Dutta HK, Mathur M, Bhatnagar V. A histopathological study of esophageal atresia and tracheoesophageal fistula. *J Pediatr Surg* 2000;35:438–41.
36. Pederiva F, Burgos E, Francica I, et al. Intrinsic esophageal innervation in esophageal atresia without fistula. *Pediatr Surg Int* 2008;24:95–100.